Toward Practical Aerodynamic Design Through Numerical Optimization

David W. Zingg,* and Laura Billing,†
Institute for Aerospace Studies, University of Toronto
4925 Dufferin St., Toronto, Ontario M3H 5T6, Canada

A Newton-Krylov algorithm for aerodynamic optimization is applied to the multipoint design of an airfoil for eighteen different operating conditions. The operating conditions include four cruise conditions and four long-range cruise conditions at maximum and minimum cruise weights and altitudes. In addition, eight operating points are included in order to provide adequate maneuvering capabilities under dive conditions at the same maximum and minimum weights and altitudes with two different load factors. Finally, two low-speed operating conditions are included at the maximum and minimum weights. The problem is posed as a multipoint optimization problem with a composite objective function that is formed by a weighted sum of the individual objective functions. The Newton-Krylov algorithm, which employs the discrete-adjoint method, has been extended to include the lift constraint among the governing equations, leading to an improved lift-constrained drag minimization capability. The optimized airfoil performs well throughout the flight envelope. This example demonstrates how numerical optimization can be applied to practical aerodynamic design.

I. Introduction

Beginning with the work of Hicks et al.[1] and Hicks and Henne,[2] numerical algorithms for aerodynamic optimization based on computational fluid dynamics have progressed rapidly over the past thirty-odd years. The introduction of adjoint methods by Pironneau[3] and Jameson[4] greatly improved the efficiency of gradient-based algorithms.[5–9] Numerical optimization provides the following capabilities to aid the designer:

- a rapid search of the design space for the optimum;
- a thorough understanding of trade-offs;
- rapid evaluation and comparison of competing concepts;
- the ability to produce aerodynamic shapes that formerly required extensive aerodynamic expertise, such as the Liebeck sections of the 1970's,[10] which were redesigned using optimization by Driver and Zingg[11] without exploiting any knowledge of Stratford pressure recovery.

The designer must provide a complete specification of the optimization problem, including off-design conditions for which there are specific requirements.

Most papers describing aerodynamic optimization algorithms contain examples of single-point optimizations, i.e. an airfoil or wing is optimized for one operating condition. While this is useful for proving the effectiveness of the optimization algorithm, single-point optimization is rarely the best approach for a practical design. A wing must be able to operate efficiently in several different areas of the flight envelope. While it is accepted that flaps and possibly slats be deployed for take-off, climb, and landing, a single wing shape is used for most other conditions. For example, a wing must operate over a range of flight Mach numbers and a range of lift coefficients. In addition, satisfactory performance is required under dive and high-lift

*Professor, Senior Canada Research Chair in Computational Aerodynamics, Associate Fellow AIAA.
†Graduate Student

conditions. This leads to a complex multipoint multi-objective optimization problem, and the resulting wing's performance at a given condition is compromised by the need for good performance under other conditions. In order to achieve a design that is truly optimal with respect to the designer's priorities without being constrained by any assumptions that may not be applicable, the design problem must be specified much more precisely and completely than previously. This requires the designer to place more emphasis on the definition of off-design requirements, which in turn will necessitate a deeper quantitative understanding of uncertainties and risks. More stringent off-design requirements will compromise on-design performance; therefore, it is important that the off-design requirements not be excessively stringent.

In this paper we apply a Newton-Krylov algorithm for aerodynamic shape optimization based on the Reynolds-averaged Navier-Stokes equations known as Optima2D[8,9] to a complex eighteen-point airfoil optimization problem involving both on- and off-design operating conditions. The objective is to demonstrate how to apply optimization to practical aerodynamic design. Although the present example is itself not a practical design, since manufacturing and structural constraints are not considered in detail, further operating requirements may be needed, and three-dimensional and laminar-turbulent transition effects are not considered, it contains the key elements of a practical design and therefore provides a suitable platform to investigate the issues associated with the application of aerodynamic optimization to practical problems.

II. Newton-Krylov Algorithm For Aerodynamic Shape Optimization

The Newton-Krylov approach of Nemec and Zingg[8,9] is briefly described. For a complete description of Optima2D, see Nemec.[12] The geometry is parameterized through B-splines. The vertical coordinates of the B-spline control points are the design variables for the optimization. Depending on the objective function, the angle of attack can also be a design variable. The compressible Navier-Stokes equations are solved with a Newton-Krylov method in which the linear system arising at each Newton iteration is solved using the generalized minimal residual method (GMRES) preconditioned with an incomplete lower-upper (ILU) factorization of an approximate Jacobian matrix with limited fill. The Spalart-Allmaras turbulence model is used to compute the eddy viscosity. The spatial derivatives in the governing equations are discretized using second-order centered finite differences with added scalar numerical dissipation through a curvilinear coordinate transformation. The gradient is calculated using the discrete adjoint method; solution of the adjoint equation is accomplished through the same preconditioned Krylov method. Geometric constraints are added to the objective function as penalty terms. A new set of design variables is computed using a quasi-Newton optimizer in which an estimate of the inverse Hessian based on the BFGS (Broyden-Fletcher-Goldfarb-Shanno) rank-two update formula is used to compute a search direction.[13] The step size is determined using a line search, which terminates when the strong Wolfe conditions are satisfied.[13] Each time a new shape is calculated, the initial grid is perturbed using a simple algebraic technique.

The handling of a lift constraint in Optima2D has been improved. Previously, this constraint was lifted into the objective function in the same manner as the geometric constraints, and the angle of attack was included among the design variables. The lift constraint is now treated as one of the governing equations. The equation for the lift coefficient constraint is added to the residual vector for the discretized flow equations. The angle of incidence is added to the vector of conservative flow variables and is no longer a design variable. For the flow solution, the matrix-vector products needed by GMRES are obtained in a matrix-free manner. Therefore, the additional entries in the Jacobian matrix associated with the partial derivatives of the lift coefficient constraint with respect to the flow variables and the angle of incidence and the partial derivatives of the flow equations with respect to the angle of incidence appear automatically. The approximate Jacobian matrix used to form the ILU preconditioner is based on nearest neighbour contributions only, so only the partial derivative of the lift constraint with respect to the angle of incidence is required. This is determined analytically. In order to compute accurate gradients, all of the additional entries in the Jacobian are determined analytically for the calculation of the adjoint variables. For details, see Billing.[14]

The accuracy of the flow solver has been studied extensively.[15] The optimization is performed using a relatively coarse mesh which can be expected to produce drag coefficients that are substantially higher than the grid converged values. However, differences in drag are predicted very accurately. Therefore, we have a high degree of confidence in the optimized airfoil, which is subsequently analyzed using a much finer mesh.

Table 1. Operating conditions for eighteen-point optimization.

Operating Point	Reynolds Number	Mach Number	Lift Coefficient
A	27.32×10^6	0.72	0.17
B	27.32×10^6	0.72	0.28
C	18.57×10^6	0.72	0.27
D	18.57×10^6	0.72	0.45
E	24.22×10^6	0.64	0.21
F	24.22×10^6	0.64	0.36
G	16.46×10^6	0.64	0.34
H	16.46×10^6	0.64	0.57
I	28.88×10^6	0.76	0.28
J	28.88×10^6	0.76	0.15
K	28.88×10^6	0.76	0.46
L	28.88×10^6	0.76	0.25
M	19.62×10^6	0.76	0.45
N	19.62×10^6	0.76	0.24
O	19.62×10^6	0.76	0.74
P	19.62×10^6	0.76	0.40
Q	11.8×10^6	0.16	–
R	15.0×10^6	0.20	–

III. Design Problem Definition

In order to define a practical multipoint optimization problem, we consider a hypothetical aircraft with a maximum weight of 100,000 lbs., a wing area of 1000 square feet, and a maximum cruise Mach number of 0.88. We consider the section at the mean aerodynamic chord and assume that the sectional lift coefficient is equal to the wing lift coefficient. The target thickness to chord ratio is 0.14. The operating conditions on which the multipoint optimization is based are cruise, long-range cruise, maneuvering under dive conditions, and low-speed performance.

The first four operating conditions, labelled A–D in Table 1, correspond to cruise. The effective Mach number is 0.72, based on a sweep angle of 35 degrees. For operating point A the altitude is 29,000 feet, the weight is 60,000 lbs.; for B the altitude is the same, but the weight is 100,000 lbs.; for C the altitude is 39,000 feet, the weight is 60,000 lbs.; for D the altitude is 39,000 feet, the weight is 100,000 lbs. This leads to the Reynolds numbers and lift coefficients given in Table 1. The objective for these four operating points is to minimize the drag while maintaining the specified lift coefficient.

The next four operating conditions, labelled E–H, correspond to long-range cruise. The altitudes and weights are the same as for A–D respectively. The Mach number is 0.78, producing an effective Mach number of 0.64. The objective function is to maximize the product of the Mach number and the lift-to-drag ratio. Since the Mach number and the lift coefficient are specified, this again requires that the drag coefficient be minimized.

The next eight operating conditions (I–P) are associated with the requirement for maneuvering under dive conditions. The Mach number is 0.93, the effective Mach number 0.76. For operating point I, the altitude is 29,000 ft., the weight 60,000 lbs., and the load factor is 1.3. For operating point J, the altitude and weight are the same, but the load factor is 0.7. Operating points K and L have an altitude of 29,000 ft., a weight of 100,000 lbs., and load factors 1.3 and 0.7, respectively. For operating points M and N, the altitude is 39,000 ft., the weight is 60,000 lbs., and the load factors are 1.3 and 0.7, respectively. Operating points O and P have the same altitude and load factors, but the weight is 100,000 lbs. The objective is to keep shock strengths modest, such that the upstream Mach number at all shocks is less than 1.35. The actual objective function used is lift-constrained drag minimization, since this tends to weaken or eliminate

shocks.

The final two operating points require an adequate maximum lift coefficient at low speed conditions. For operating condition Q, the altitude is sea level, the weight is 60,000 lbs., and the effective Mach number is 0.16. For operating point R the weight is 100,000 lbs., and the effective Mach number is 0.20. The objective is to ensure that the maximum lift coefficient under these conditions is at least 1.75.

The first eight cases, A–H, represent multiple, potentially competing, objectives. A complete problem specification could involve some sort of prioritization of these operating conditions based on the aircraft mission requirements. For this study we assume that they are all of equal importance. The last ten cases, I-R, can be considered constraints. If the targets are satisfied, there is no particular benefit to exceeding them.

These eighteen operating points span the flight envelope. However, there is no guarantee that good performance under these particular operating conditions will lead to adequate performance under intermediate conditions. Furthermore, some of these operating points may be redundant, i.e. adequate performance at these points can be achieved even if they are excluded from the composite objective function. Neither the operating points needed to achieve optimal performance throughout the flight envelope nor the appropriate weights are known a priori. Therefore, we begin with equal weights and modify them as the optimization progresses. This is further discussed below. Zingg and Elias[16] have developed an automated procedure for determining operating points and their weights. It would be worthwhile to extend this procedure to more complicated multipoint optimization problems such as the current eighteen-point optimization.

IV. Multipoint Optimization

The geometry is parameterized using 15 B-spline control points, with the NACA 0015 as the initial geometry. Three control points are frozen at the leading edge and two at the trailing edge. Hence there are ten design variables, five on each surface. A floating thickness constraint of 14.2% chord is imposed to ensure a thickness of at least 14% chord. In addition, a thickness of 1% chord is imposed at 95% chord and 0.2% at 99% chord in order to prevent crossover. The meshes used have a C topology with 289 nodes in the streamwise direction and 65 in the normal direction; the off-wall spacing is 1×10^{-6} chords. Fully turbulent flow is assumed.

For operating points A through P, the objective is lift-constrained drag minimization; this is accomplished using the new approach for handling the lift constraint described in Section II. The objective function is the drag coefficient normalized by the drag coefficient of the initial geometry at the specified operating conditions. The objective function for operating points Q and R is given by:

$$J = \left(1 - \frac{C_l}{C_l^*}\right)^2 \tag{1}$$

where C_l^* is a target lift coefficient. In order to maximize the maximum lift coefficient, a target lift coefficient is chosen that is somewhat higher than can be achieved, and the angle of attack is included among the design variables. This objective function is again normalized by the initial value.

A composite objective function is formed by a weighted sum of the individual objective functions, which include the thickness constraints, as follows:

$$J = \omega_A J_A + \omega_B J_B + \ldots + \omega_R J_R \tag{2}$$

where the subscripts indicate the operating points, and the ω's are the weights. The normalization of the individual objective functions by their initial values is important in forming the composite objective function. If this is not done, the objective functions associated with lift maximization will greatly exceed those associated with drag minimization and can dominate the gradient. In order to determine suitable values for the weights, the optimization proceeds in four steps. The objective function for each operating condition is initially assigned a weight of unity. The multipoint optimization is then run to convergence. If the drag coefficient for any of operating points A through H is not significantly decreased, the corresponding weight is increased. This is repeated three times (steps 2, 3, and 4). During the fourth step, the weights on any of operating conditions I through R that do not meet their targets are also increased. The weights for each step are listed in Table 2. This process could be continued until precise goals are met with respect to the relative performance at each operating condition. However, the four steps presented are sufficient

Table 2. Weights used in the composite objective function for each optimization step.

Operating Point	1	2	3	4
A	1.0	1.5	1.5	1.5
B	1.0	1.5	1.5	1.5
C	1.0	1.5	1.5	1.5
D	1.0	2.0	3.0	3.0
E	1.0	2.0	3.0	4.0
F	1.0	1.5	2.5	2.5
G	1.0	1.5	2.5	2.5
H	1.0	1.0	1.2	1.2
I	1.0	1.0	1.0	1.0
J	1.0	1.0	1.0	1.0
K	1.0	1.0	1.0	1.0
L	1.0	1.0	1.0	1.0
M	1.0	1.0	1.0	1.0
N	1.0	1.0	1.0	1.0
O	1.0	1.0	1.0	8.0
P	1.0	1.0	1.0	1.0
Q	1.0	1.0	1.0	5.0
R	1.0	1.0	1.0	5.0

Figure 1. Designed airfoil section

to demonstrate the process and to produce an airfoil that generally performs as desired. The weights for operating points A through H are determined by the requirement that at each operating point the drag coefficient must be significantly lower than the initial value. This is somewhat arbitrary, and other criteria could be used.

Table 3 summarizes the performance of the resulting airfoil, which is depicted in Fig. 1. The airfoil shape has no undesirable features despite the absence of curvature constraints. The drag coefficients are reasonably low for operating points A through H, and all of the off-design targets are satisfied. Note that these drag coefficients are computed on a coarse mesh and are much higher than those computed on a finer mesh, which are reported below. For some of the off-design operating conditions, the performance exceeds the requirement. This indicates either that the weight on this point is too high or that the point is not critical, i.e. satisfactory performance is achieved even if the point is given zero weight. In the former case, a reduction in the weight could lead to an improvement at the on-design operating points (A-H). However, such an improvement is likely to be small, since the most difficult off-design condition (operating point O) is the critical one, and it is just barely satisfied. Overall, the airfoil designed using the eighteen-point optimization provides excellent performance over the entire range of operating conditions. Pressure distributions for operating points A-H are shown in Figs. 2 and 3. The solutions are shock-free at all eight operating points.

Table 3. Performance of airfoil designed through eighteen-point optimization. The maximum Mach number column gives the maximum local Mach number upstream of a shock wave.

Operating Point	C_l	C_d	Maximum Mach Number	$C_{l\max}$
A	0.17	0.0125	–	–
B	0.28	0.0126	–	–
C	0.27	0.0128	–	–
D	0.45	0.0134	–	–
E	0.21	0.0122	–	–
F	0.36	0.0125	–	–
G	0.34	0.0126	–	–
H	0.57	0.0136	–	–
I	0.28	0.0139	1.19	–
J	0.15	0.0143	1.26	–
K	0.46	0.0171	1.28	–
L	0.25	0.0138	1.17	–
M	0.45	0.0170	1.27	–
N	0.24	0.0139	1.17	–
O	0.74	0.0562	1.34	–
P	0.40	0.0158	1.25	–
Q	–	–	–	1.77
R	–	–	–	1.78

The requirements of operating points O, Q, and R significantly compromise the performance at operating points A-H. This emphasizes the importance of careful specification of off-design performance requirements. Another interesting observation based on Table 3 is that the drag coefficient at operating point O is high, indicating shock-induced turbulent boundary-layer separation. This suggests that the target for the Mach number upstream of shocks for operating points I through P should perhaps be reduced. However, it must be recognized that this will penalize the performance at operating points A through H and therefore should only be done if there is a good reason to do so.

When performing aerodynamic optimization based on specific points in the operating envelope, one must ensure that performance is also satisfactory at intermediate operating conditions not represented in the composite objective function. If unsatisfactory performance is found, additional operating points must be added and the optimization repeated. Fig. 4 displays the variation of the drag coefficient with Mach number at fixed values of lift coefficient for the designed airfoil for Mach numbers ranging from 0.60 to 0.78 and lift coefficients from 0.10 to 0.80. Similarly, Fig. 5 shows the variation of the drag coefficient with lift coefficient at fixed Mach number. For both figures, the Reynolds number is 20 million. These results were computed on a fine mesh with 579 nodes in the streamwise direction and 130 in the normal direction and an off-wall normal spacing of 5×10^{-7} chords. Performance throughout this range of Mach numbers and lift coefficients is consistent with that at the operating points included in the composite objective function. Consequently, no additional operating points need to be added. Furthermore, the drag coefficients computed on the fine mesh are much lower than those computed on the coarse mesh used for optimization. The reason that consistent aerodynamic performance of the airfoil is found throughout the flight envelope, even at operating points that are not part of the optimization, is that for this example the number of operating points and constraints used in the optimization substantially exceeds the number of design variables. Consequently, the optimizer does not have the freedom to produce substantial improvements at the specific operating points without improving the performance throughout the flight envelope.

Fig. 6 displays the low-speed performance of the optimized airfoil at a Mach number of 0.20 and a Reynolds number of ten million computed on the fine mesh. The maximum lift coefficient is 2.05 at an angle

of attack of 18.5 degrees. This exceeds the target maximum lift coefficient; hence the weights on operating points Q and R can be reduced.

V. Conclusions

We have presented an eighteen-point optimization problem that serves as an example of a practical aerodynamic design problem, thereby demonstrating a methodology for performing aerodynamic design using numerical optimization and revealing many of the issues which arise. Overall, the Newton-Krylov approach to multipoint optimization, which is based on a composite objective function with user-specified weights that evolve over several optimization steps, is seen to be effective. The resulting optimized airfoil performs well throughout the prescribed flight envelope. In order to fully exploit this optimization capability, desired aerodynamic performance must be completely prescribed throughout the flight envelope, and off-design requirements must be precisely specified based on a thorough understanding of uncertainties and risks.

It is desirable to automate the weight selection process; therefore, future work will concentrate on extending the ideas of Zingg and Elias[16] to complex multipoint problems such as that presented here. Furthermore, it is of interest to extend the present optimization capability to three dimensions in order to facilitate the design of wings and complete aircraft.

Acknowledgments

Many thanks to Dr. Tom Nelson of Bombardier Aerospace for suggesting this multipoint airfoil design case. Thanks also to Xun Huan and Beckett Zhou for performing numerous computations for the optimized airfoil. The funding of the first author by the Natural Sciences and Engineering Research Council of Canada and the Canada Research Chairs program and the second author by the Natural Sciences and Engineering Research Council of Canada is gratefully acknowledged.

References

[1]Hicks, R.M. and Murman, E.M. and Vanderplaats, G.N., "An assessment of airfoil design by numerical optimization," TM X-3092, NASA, July, 1974.

[2]Hicks, R.M. and Henne, P.A., "Wing design by numerical optimization", *J. of Aircraft*, vol. 3, pp. 407-412, 1978.

[3]Pironneau O., "On optimum design in fluid mechanics," *J. Fluid Mech.*, vol. 64, pp. 97-110, 1974.

[4]Jameson A., "Aerodynamic design via control theory," *J. of Scientific Computing*, vol. 3, no. 3, pp. 233-260, 1988.

[5]Elliott, J. and Peraire, J., "Practical 3D aerodynamic design and optimization using unstructured meshes," *AIAA J.*, vol. 35, pp. 1479-1485, 1997.

[6]Reuther, J.J. and Jameson, A. and Alonso, J.J. and Rimlinger, M.J. and Saunders, D., "Constrained multipoint aerodynamic shape optimization using an adjoint formulation and parallel computers, part 1," *J. of Aircraft*, vol. 36, pp. 51-60, 1999.

[7]Nielsen, E.J. and Anderson, W.K., "Aerodynamic design optimization on unstructured meshes using the Navier-Stokes equations," *AIAA J.*, vol. 37, pp. 1411-1419, 1999.

[8]Nemec, M., and Zingg, D.W., "Newton-Krylov algorithm for aerodynamic design using the Navier-Stokes equations," *AIAA J.*, Vol. 40, No. 6, 2002, pp. 1146-1154.

[9]Nemec, M., Zingg, D.W., and Pulliam, T.H., "Multipoint and multi-objective aerodynamic shape optimization," *AIAA J.*, Vol. 42, No. 6, 2004, pp. 1057-1065.

[10]Liebeck, R. H., "A class of airfoils designed for high lift in incompressible flow," *Journal of Aircraft*, Vol. 10, No. 10, 1973, pp. 610–617.

[11]Driver, J., and Zingg, D.W., "Optimized natural-laminar-flow airfoils," AIAA Paper 2006-247, 2006.

[12]Nemec, M., "Optimal shape design of aerodynamic configurations: a Newton-Krylov approach," Ph.D. Thesis, University of Toronto Institute for Aerospace Studies, 2002.

[13]Nocedal, J. and Wright, S.J., *Numerical Optimization*, Springer-Verlag, New York, 1999.

[14]Billing, L.K., "On the development of an improved lift-constrained aerodynamic optimization algorithm," M.A.Sc. Thesis, University of Toronto Institute for Aerospace Studies, 2006.

[15]Zingg, D.W., "Grid studies for thin-layer-Navier-Stokes computations of airfoil flowfields," Tech. Note, *AIAA J.*, Vol. 30, No. 10, pp. 2561-2564, 1992.

[16]Zingg, D.W., and Elias, S., "On aerodynamic optimization under a range of operating conditions," AIAA Paper 2006-1053, Jan. 2006.

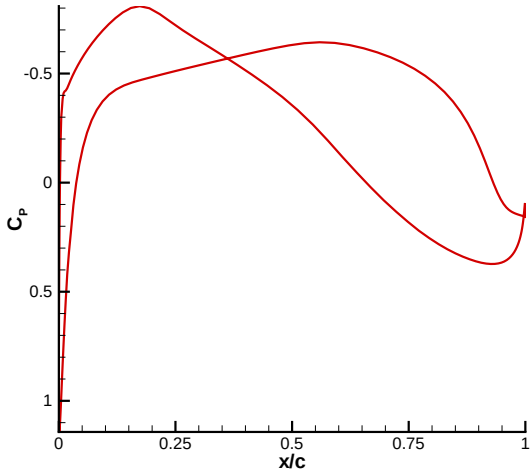

(a) Point A

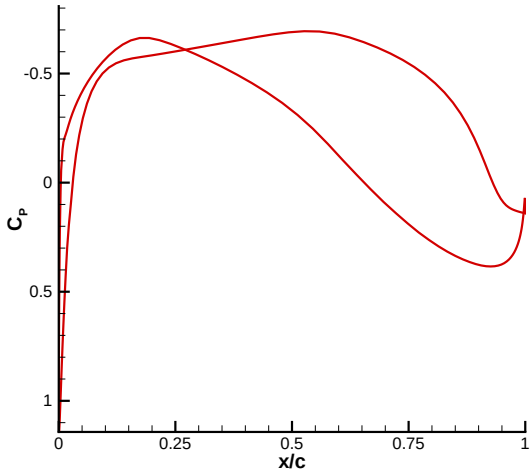

(b) Point B

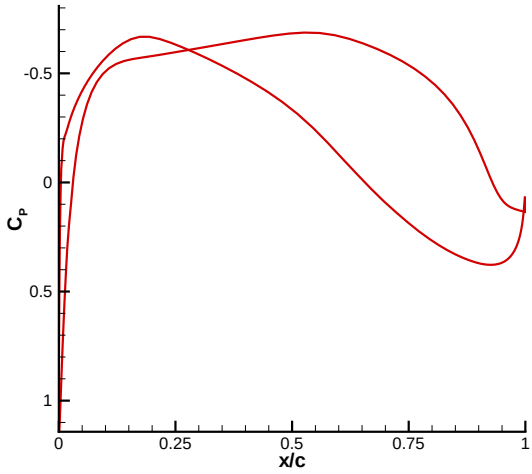

(c) Point C

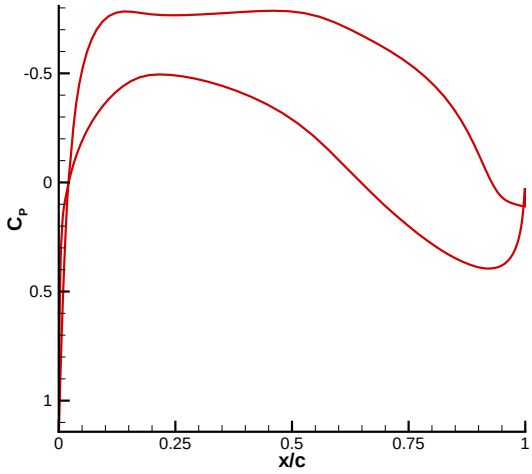

(d) Point D

Figure 2. Surface pressure coefficient distributions for operating points A–D.

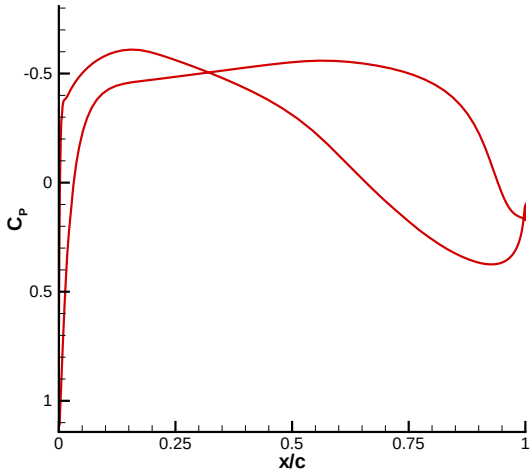

(a) Point E

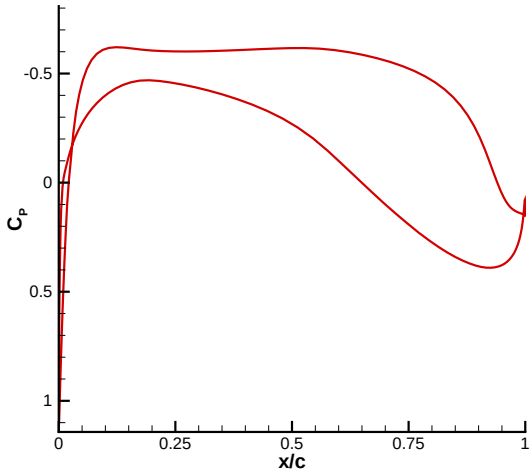

(b) Point F

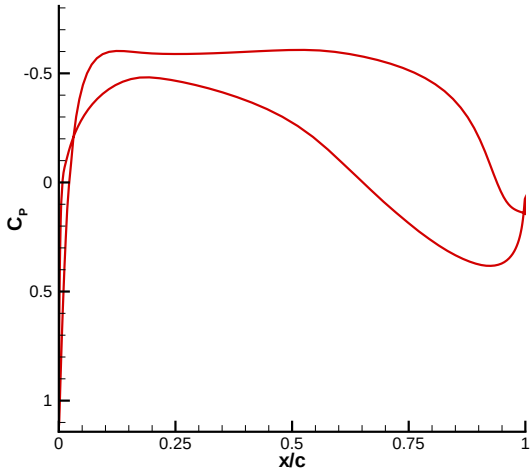

(c) Point G

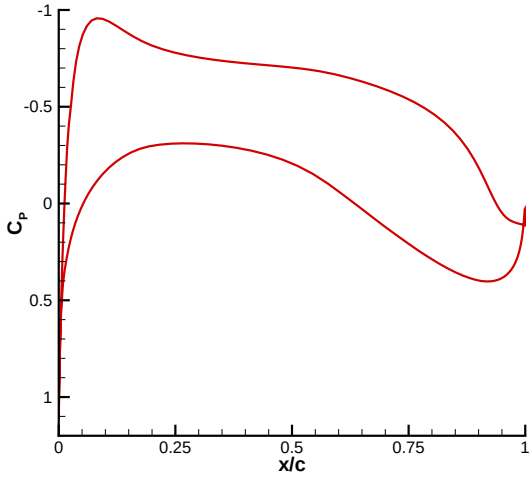

(d) Point H

Figure 3. Surface pressure coefficient distributions for operating points E–H.

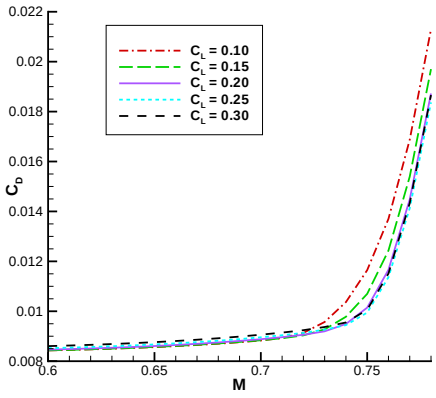

(a) $C_L = 0.10,\ 0.15,\ 0.20,\ 0.25,\ 0.30$

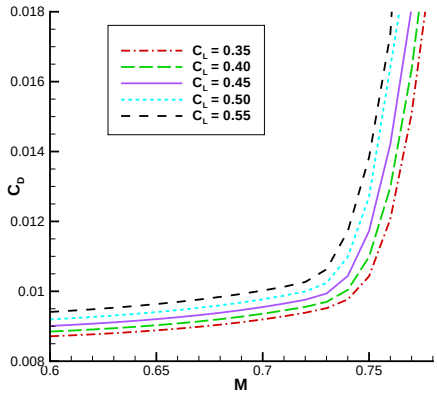

(b) $C_L = 0.35,\ 0.40,\ 0.45,\ 0.50,\ 0.55$

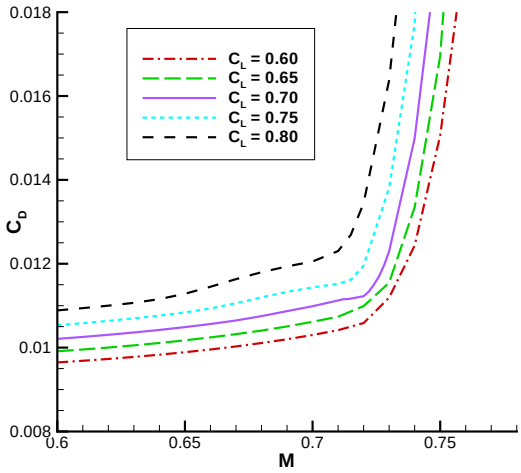

(c) $C_L = 0.60,\ 0.65,\ 0.70,\ 0.75,\ 0.80$

Figure 4. Drag coefficient vs. Mach number at various values of the lift coefficient for the designed airfoil at a Reynolds number of 20 million.

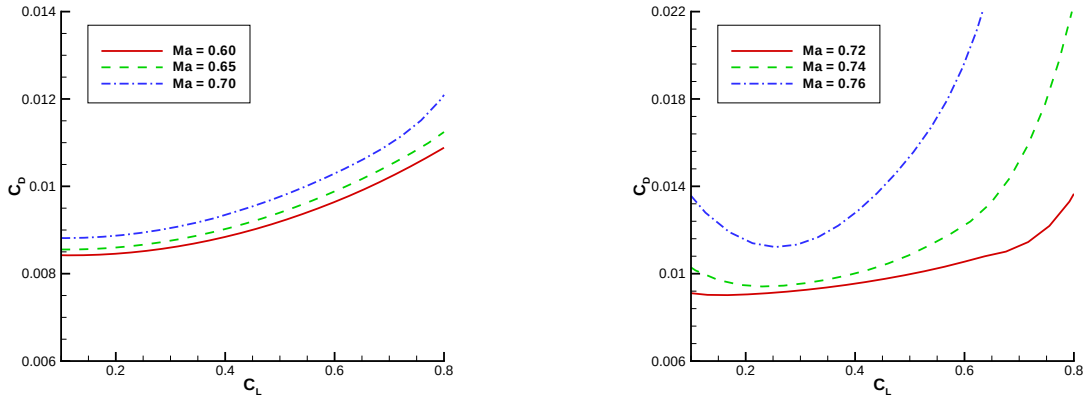

(a) $Ma = 0.60,\ 0.65,\ 0.70$

(b) $Ma = 0.72,\ 0.74,\ 0.76$

Figure 5. Drag coefficient vs. lift coefficient at various values of Mach number for the designed airfoil at a Reynolds number of 20 million.

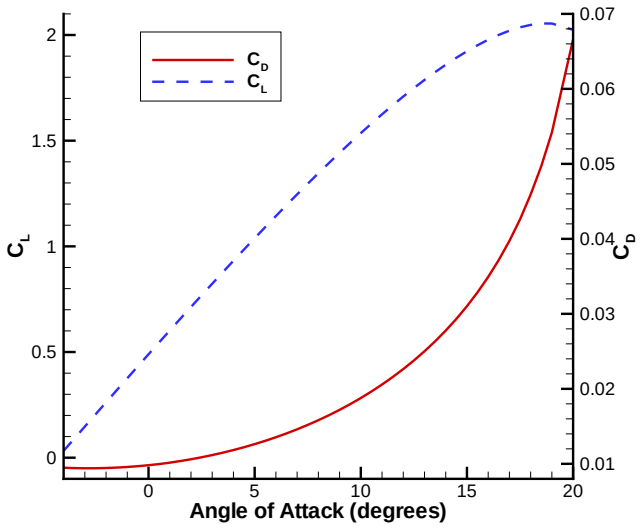

Figure 6. Lift and drag coefficients vs. angle of attack at a Mach number of 0.20 and a Reynolds number of ten million